

ARMY RESEARCH LABORATORY



Photoacoustic Spectroscopy for Chemical Detection

by Ellen L. Holthoff and Paul M. Pellegrino

ARL-RP-0410

September 2012

A reprint from *Proceedings of SPIE, CBRNE Sensing*

NOTICES

Disclaimers

The findings in this report are not to be construed as an official Department of the Army position unless so designated by other authorized documents.

Citation of manufacturer's or trade names does not constitute an official endorsement or approval of the use thereof.

Destroy this report when it is no longer needed. Do not return it to the originator.

Army Research Laboratory

Adelphi, MD 20783-1197

ARL-RP-0410

September 2012

Photoacoustic Spectroscopy for Chemical Detection

Ellen L. Holthoff and Paul M. Pellegrino
Sensors and Electron Devices Directorate, ARL

A reprint from *Proceedings of SPIE, CBRNE Sensing*

REPORT DOCUMENTATION PAGE				Form Approved OMB No. 0704-0188
<p>Public reporting burden for this collection of information is estimated to average 1 hour per response, including the time for reviewing instructions, searching existing data sources, gathering and maintaining the data needed, and completing and reviewing the collection information. Send comments regarding this burden estimate or any other aspect of this collection of information, including suggestions for reducing the burden, to Department of Defense, Washington Headquarters Services, Directorate for Information Operations and Reports (0704-0188), 1215 Jefferson Davis Highway, Suite 1204, Arlington, VA 22202-4302. Respondents should be aware that notwithstanding any other provision of law, no person shall be subject to any penalty for failing to comply with a collection of information if it does not display a currently valid OMB control number.</p> <p>PLEASE DO NOT RETURN YOUR FORM TO THE ABOVE ADDRESS.</p>				
1. REPORT DATE (DD-MM-YYYY)	2. REPORT TYPE			3. DATES COVERED (From - To)
September 2012				
4. TITLE AND SUBTITLE				5a. CONTRACT NUMBER
Photoacoustic Spectroscopy for Chemical Detection				5b. GRANT NUMBER
				5c. PROGRAM ELEMENT NUMBER
				5d. PROJECT NUMBER
6. AUTHOR(S)				5e. TASK NUMBER
Ellen L. Holthoff and Paul M. Pellegrino				5f. WORK UNIT NUMBER
7. PERFORMING ORGANIZATION NAME(S) AND ADDRESS(ES)				8. PERFORMING ORGANIZATION REPORT NUMBER
U.S. Army Research :Laboratory ATTN: RDRL-SEE-E 2800 Powder Mill Road Adelphi, MD 20783-1197				ARL-RP-0410
9. SPONSORING/MONITORING AGENCY NAME(S) AND ADDRESS(ES)				10. SPONSOR/MONITOR'S ACRONYM(S)
				11. SPONSOR/MONITOR'S REPORT NUMBER(S)
12. DISTRIBUTION/AVAILABILITY STATEMENT				
Approved for public release; distribution unlimited.				
13. SUPPLEMENTARY NOTES				
14. ABSTRACT				
The Global War on Terror has made rapid detection and identification of chemical and biological agents a priority for Military and Homeland Defense applications. Reliable real-time detection of these threats is complicated by our enemy's use of a diverse range of materials. Therefore, an adaptable platform is necessary. Photoacoustic spectroscopy (PAS) is a useful monitoring technique that is well suited for trace detection of gaseous media. This method routinely exhibits detection limits at the parts-per-billion (ppb) or sub-ppb range. The versatility of PAS also allows for the investigation of solid and liquid analytes. Current research utilizes quantum cascade lasers (QCLs) in combination with an air-coupled solid-phase photoacoustic cell design for the detection of condensed phase material films deposited on a surface. Furthermore, variation of the QCL pulse repetition rate allows for identification and molecular discrimination of analytes based solely on photoacoustic spectra collected at different film depths.				
15. SUBJECT TERMS				
Photoacoustic spectroscopy, quantum cascade laser, solid-phase, depth profiling				
16. SECURITY CLASSIFICATION OF:		17. LIMITATION OF ABSTRACT	18. NUMBER OF PAGES	19a. NAME OF RESPONSIBLE PERSON Ellen L. Holthoff
a. REPORT UNCLASSIFIED	b. ABSTRACT UNCLASSIFIED	c. THIS PAGE UNCLASSIFIED	UU	13
				19b. TELEPHONE NUMBER (Include area code) (301) 394-0939

Photoacoustic Spectroscopy for Chemical Detection

Ellen L. Holthoff* and Paul M. Pellegrino

U.S. Army Research Laboratory, RDRL-SEE-E, 2800 Powder Mill Road, Adelphi, MD, 20783

ABSTRACT

The Global War on Terror has made rapid detection and identification of chemical and biological agents a priority for Military and Homeland Defense applications. Reliable real-time detection of these threats is complicated by our enemy's use of a diverse range of materials. Therefore, an adaptable platform is necessary. Photoacoustic spectroscopy (PAS) is a useful monitoring technique that is well suited for trace detection of gaseous media. This method routinely exhibits detection limits at the parts-per-billion (ppb) or sub-ppb range. The versatility of PAS also allows for the investigation of solid and liquid analytes. Current research utilizes quantum cascade lasers (QCLs) in combination with an air-coupled solid-phase photoacoustic cell design for the detection of condensed phase material films deposited on a surface. Furthermore, variation of the QCL pulse repetition rate allows for identification and molecular discrimination of analytes based solely on photoacoustic spectra collected at different film depths.

Keywords: Photoacoustic spectroscopy, quantum cascade laser, solid-phase, depth profiling

1. INTRODUCTION

The rapid detection and identification of hazardous materials (i.e., chemical, biological, energetic) deposited on surfaces is of great importance for military and homeland defense applications. A non-destructive method for determining the composition of unknown materials deposited on a surface, as well as discrimination between the material and the surface, is an attractive analysis tool. Photoacoustic spectroscopy (PAS) offers unique capabilities for investigating condensed phase samples due to its simplicity and resistance to scattering effects, which is often an issue associated with other common techniques such as infrared (IR) reflectance spectroscopy.^{1, 2} Additionally, PAS, as well as other photothermal techniques, have proven advantageous for depth profiling, as they offer a frequency dependent, and therefore adjustable, probe depth.

Photothermal spectroscopy encompasses a group of highly sensitive methods that can be used to detect trace levels of optical absorption and subsequent thermal perturbations of the sample in gas, liquid or solid phases. The underlying principle that connects these various spectroscopic methods is the measurement of physical changes (i.e., temperature, density, or pressure) as a result of a photo-induced change in the thermal state of the sample. Examples of photothermal techniques include photothermal interferometry (PTI), photothermal lensing (PTL), photothermal deflection (PTD), and PAS. All photothermal processes consist of several linked steps that result in a change of the state of the sample. In comparison to other photothermal techniques, which measure the refractive index using combinations of probe sources and detectors, PAS measures the pressure wave produced by sample heating.³ Successful applications of PAS in gases and condensed matter have made this a notable technique.

Investigating solid samples using the photoacoustic technique is advantageous as it allows optical absorption measurements to be made for optically opaque samples and is insensitive to scattered light. This unique capability of photoacoustic spectroscopy for the investigation of condensed phase samples is attractive,⁴⁻⁷ especially in comparison to commonly used passive IR reflectance techniques. Reflectance data can depend strongly on the refractive index of the sample, the particle size and size distribution, packing density, and sample homogeneity.² The surface on which the sample is deposited may also interfere with the collection of a quality reflectance spectrum. In contrast, PAS allows for discrimination between the sample and surface or different sample layers. PAS of condensed phase samples is also often applied to depth profiling of layered samples and two- and three-dimensional tomographic imaging for biomedical applications.⁸⁻¹⁰ Although there have been several reports discussing the use of tunable infrared sources, such as quantum cascade lasers (QCLs) and CO₂ lasers, to obtain photoacoustic spectra of gases,¹¹⁻¹⁸ the application of these sources in photoacoustic experiments on condensed phase samples are minimal.^{7, 19, 20} In this current work, we report on the use of a continuously tunable pulsed QCL, in combination with a photoacoustic cell designed for solid and liquid

samples, for the identification of urea and 2,4,6-trinitrotoluene (TNT) deposited on a surface. We also investigate glycerol films deposited on a substrate, and discrimination between this compound and the substrate itself based on sample depth profiling. These materials were chosen specifically for this proof of concept demonstration because each has known absorbance features in the wavelength tuning range of the QCL.

2. THEORY

Early work by Kreuzer demonstrated the analytic power of PAS in gases, but the technique can also be applied readily to liquids and solids.^{15, 21-23} PAS in these phases can be accomplished using both a direct or indirect coupling method. Direct coupling is the most straightforward and, as the name implies, the acoustic wave generated in the sample is detected by a transducer in direct contact with the solid or liquid sample. Since the acoustic wave generated in the sample never crosses a high acoustical impedance interface, it is easily detected by the transducer. In comparison, indirect coupling methods are not as straightforward. Usually there is a large acoustical impedance at the sample-gas interface such that most acoustic energy will be reflected back into the sample. The indirect photoacoustic detection of liquids or solids relies on the gas-coupling method and is explained clearly by Rosencwaig as the gas-piston model.²⁴ In this model the periodic heating of the sample occurs in the absorption length of the sample, but only the heat within a diffusion length μ_s from the sample interface that is in phase with the excitation light can interact with the layer of gas directly above the surface, where

$$\mu_s = [D_s/(\pi f)]^{1/2} \quad (1)$$

and f is the modulation or pulse frequency of the excitation source, and D_s is the thermal diffusivity in the sample.²⁵ The periodic expansion in this gas layer produces an acoustic wave that can be detected using standard gas-phase microphones. μ_s is frequency dependent such that lower modulation or pulse frequencies result in longer diffusion lengths, and higher modulation or pulse frequencies result in shorter diffusion lengths.

3. EXPERIMENTAL

3.1 Reagents and Materials

Urea ($\geq 99\%$ purity), glycerol ($\geq 99\%$), methanol (MeOH, HPLC grade, 99.9%) and H₂O were purchased from Sigma-Aldrich. A solution of TNT in acetonitrile was purchased from Cerilliant (ERT-107S, 10 mg/mL, 99.9%). A urea solution was prepared from bulk material dissolved in a 2:1 MeOH:H₂O solution. Photoresist was manufactured by AZ Electronic Materials (AZ 5214-E). All chemicals were used as received unless otherwise noted. Silicon test wafers were purchased from WRS Materials (4P05-10SSP-TEST). The substrates were used as received.

3.2 Photoacoustic Measurements and Instrumentation

Figure 1 depicts a block diagram of the basic elements required for photoacoustic detection of condensed materials.

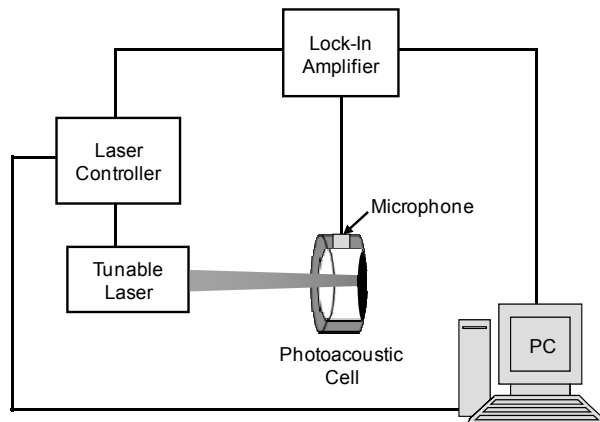


Figure 1. Schematic diagram of a general photoacoustic sensor system for the detection of condensed materials.

Quantum Cascade Laser. A broadly tunable, external cavity pulsed QCL (Daylight Solutions 11088) was employed as the excitation source for the sensing system. The laser was powered by an external controller (Daylight Solutions TLC 1001). The QCL was continuously tunable from 1015 cm^{-1} to 1240 cm^{-1} ($9.85\text{ }\mu\text{m}$ – $8.06\text{ }\mu\text{m}$) and had a spectral resolution of 1 cm^{-1} . The pulsed source operated at room temperature with convective cooling. Current pulses of 1600 mA with a $1\text{ }\mu\text{s}$ duration and pulse rate ranging from 10.0 kHz to 40.0 kHz corresponded to duty cycles of 1.0% to 4.0% and provided average optical powers of 1.60 mW to 6.50 mW , respectively.

Photoacoustic Cell. An aluminum cylindrical photoacoustic cell was fabricated in-house to meet our design specifications (0.001 in. tolerance) using standard machining techniques. The cell consisted of a 4 mm long resonator with a diameter of 16 mm . The closed cell had a zinc selenide window (Edmund Optics, model: NT63-210) on one side of the resonator and the sample substrate material on the other. The cell was equipped with a microphone (Knowles, model: FG-23629), which was wired to a power supply (AA battery) and a lock-in amplifier (via a BNC cable). Figure 2 provides a simplistic illustration and a photograph of the photoacoustic cell.

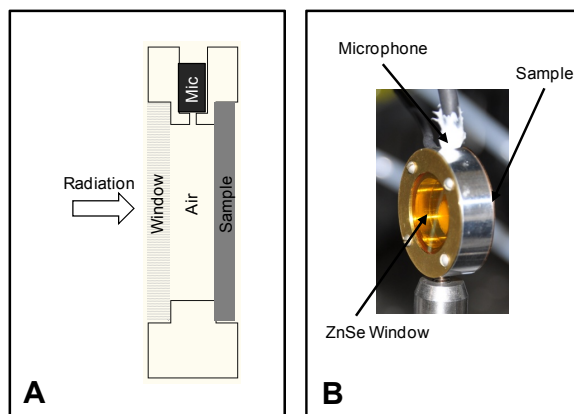


Figure 2. (A) Basic photoacoustic cell components and orientation, (B) photograph of the photoacoustic cell used when collecting data.

Data Acquisition. The signal detected by the microphone was extracted using the voltage input on a lock-in amplifier (Stanford Research Systems SR530) with a time constant of 3 s operating at the pulse frequency of the laser. LabVIEW (National Instruments, version 2009) was used to create a virtual instrument (VI) to read and record the voltage outputs from the lock-in amplifier under various conditions directly to a personal computer (PC). The VI was programmed to collect the X (in-phase), Y (quadrature), R (amplitude) and θ (phase angle) components of the photoacoustic signal. Frequency spectra were obtained by holding the laser wavelength constant while scanning the specified laser pulse frequency range. This allowed for the determination of the resonance frequencies for the photoacoustic cell. 50 measurements were made at each increment, and a mean value was calculated and recorded for the subsequent construction of a frequency spectrum. Photoacoustic spectra were obtained by holding the laser pulse frequency constant while scanning the laser wavelength range. 50 measurements were made at each increment, and a mean value was calculated and recorded for the subsequent construction of a photoacoustic spectrum. For each analyte, the photoacoustic spectrum revealed a constant background signal, attributed to the absorbance of laser radiation by the cell windows and walls.

All photoacoustic data was collected at room temperature (average $21\text{ }^{\circ}\text{C}$) and an average relative humidity of 25% .

3.3 Instrumentation

All Fourier transform infrared (FTIR) absorbance spectra were collected using a Thermo Scientific Nicolet 6700 FTIR spectrometer equipped with a potassium bromide (KBr) beamsplitter and a mercury cadmium telluride (MCT)-A (narrow band- 650 cm^{-1} cutoff) detector. A GladiATRTM (Pike Technologies) accessory was used to collect infrared spectra of solid samples using attenuated total reflectance (ATR). Each spectrum was acquired at a resolution of 2.0 cm^{-1} averaging 100 scans.

3.4 Sample Preparation

Precision micro-pipettes were used to deposit known volumes of urea and TNT solutions onto ZnSe windows. The solvent was allowed to evaporate under a fume hood, leaving solid material on the surface for spectroscopic investigations.

Photoresist was deposited onto silicon substrates using an EV Group 120 Resist Processing Cluster Tool. The pre-resist coating process included hexamethyldisilazane (HMDS) vapor wafer priming. 5 mL of the photoresist was spun cast onto the primed wafers at 2,000 rpm for 40 s. The coated wafer substrates were baked at 110 °C for 75 s. The substrates were then diced using a diamond scribing tool into 0.75 in. x 0.75 in. (1.9 cm x 1.9 cm) pieces for use in the photoacoustic cell.

A solution of 0.25% glycerol in H₂O was prepared. Volumes in increments of 100 μ L were deposited using a micropipette onto a single photoresist-coated substrate. The substrate was oriented to allow complete coverage by the glycerol/water solution. Following each deposition, the sample was stored overnight on a flat surface in the dark. Glycerol film thicknesses were calculated based on deposited material volume, average relative humidity, and substrate area.

4. RESULTS AND DISCUSSION

A frequency spectrum was collected experimentally for the photoacoustic cell. This spectrum is provided in Figure 3. The spectrum was collected as the laser frequency was continuously tuned from 10 kHz to 40 kHz, in 0.1 kHz increments. The photoacoustic cell was designed to have resonance features in this frequency range, which was limited by the operational range of the microphone. Experimental resonance frequencies of 12.5 kHz, 20.9 kHz, 26.0 kHz, and 36.3 kHz were observed for the cell. These results are in agreement with the predicted theoretical radial resonance frequencies for a cylindrical cavity resonator.^{26,27}

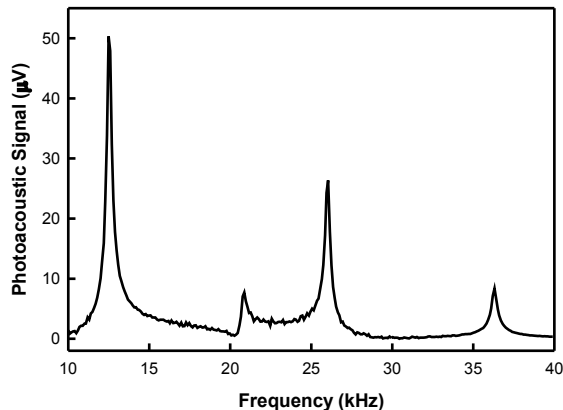


Figure 3. Measured frequency response of photoacoustic cell.

4.1 Spectroscopic Data for Energetic Samples

Laser photoacoustic spectra were collected for urea and TNT at 26.0 kHz. This frequency was chosen based on the experimental frequency data collected for the photoacoustic cell (Fig. 3) and the average laser power at this laser pulse repetition rate. The intensity-normalized spectra are provided in Figure 4. All spectra were collected as the laser continuously tuned from 1,020 cm^{-1} to 1,240 cm^{-1} (9.80 μm – 8.06 μm), in 1 cm^{-1} increments. These analytes have known absorption features in this region, assigned to primary amine (NH_2) rocking vibrations in the urea molecules,² and carbon–hydrogen (ring) in-plane bending, carbon–nitrogen and carbon–methyl (CH_3) stretching vibrations, and ring breathing found in the TNT molecules.²⁸ For both urea and TNT, there is good peak agreement between the photoacoustic and FTIR spectra. Small differences in peak frequency and bandshape between the spectra are due to refractive index effects that are often a result of ATR measurements.² The TNT spectrum collected using the FTIR exhibits a spectral feature at \sim 1030 cm^{-1} . This absorption band is not present in the photoacoustic spectrum collected for

TNT. This spectral disagreement may be due to a poor signal-to-noise ratio at the edge of the laser tuning range for this particular analyte. Furthermore, the sharp absorption feature observed at $\sim 1029\text{ cm}^{-1}$ in the photoacoustic spectrum collected for urea is also present in the spectral data found in the NIST spectral database of urea taken in Nujol.²⁹

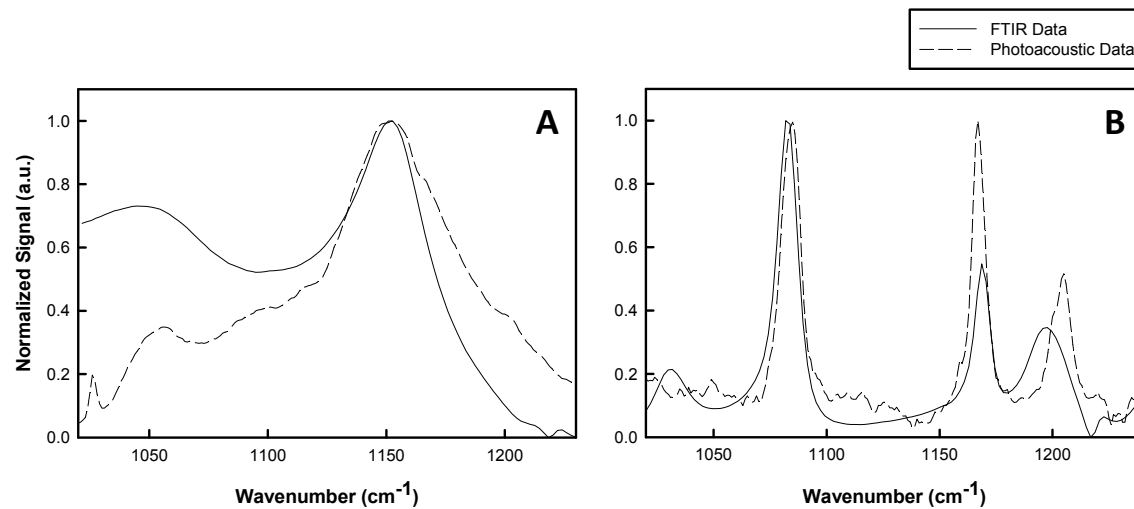


Figure 4. Measured laser photoacoustic spectrum of (A) urea; and (B) TNT compared to FTIR reference spectrum. All spectra have been intensity normalized.

4.2 Depth Profiling Investigations of Glycerol Thin Films

Laser photoacoustic spectra were collected for glycerol and photoresist. The spectra are provided in Figure 5. All spectra were collected as the laser was continuously tuned from $1,025\text{ cm}^{-1}$ to $1,240\text{ cm}^{-1}$ ($9.76\text{ }\mu\text{m}$ – $8.06\text{ }\mu\text{m}$), in 1 cm^{-1} increments. As illustrated in Figure 5, this spectral region is appealing as it contains absorption features representative of vibrational modes present in the selected molecules, specifically, carbon—oxygen stretching vibrations.² Spectral differences among glycerol and photoresist make it possible to distinguish these compounds.

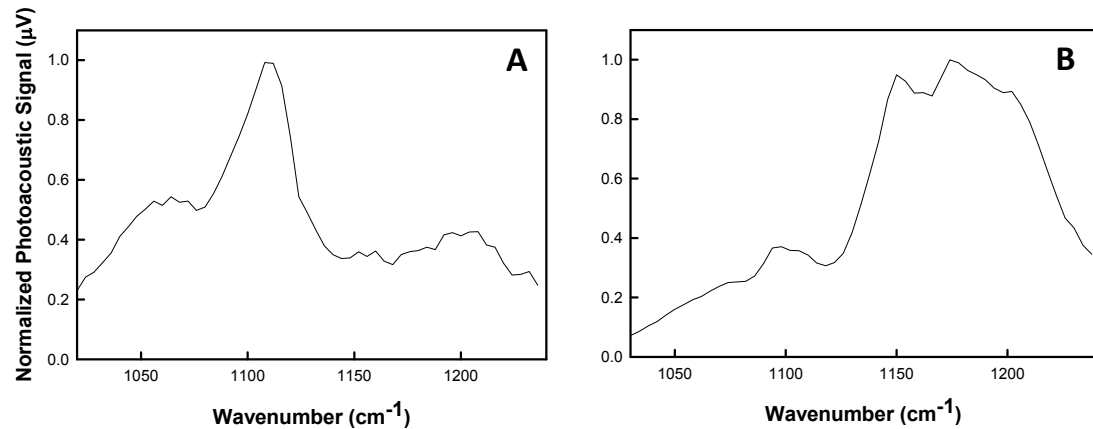


Figure 5. Measured laser photoacoustic spectrum of (A) glycerol; and (B) photoresist. The spectra have been intensity normalized.

Photoacoustic spectra collected for varying thicknesses of glycerol films on a photoresist-coated silicon substrate are shown in Figure 6. For each film thickness, spectra were 12.5 kHz. This frequency was chosen based on the experimental frequency data collected for the photoacoustic cell (Fig. 3). Using (1), the diffusion length for glycerol could be calculated at this frequency. The thermal diffusivity of glycerol can be found in the literature.³⁰ At

12.5 kHz, the calculated diffusion length from the glycerol-gas interface is 1.5 μm . Based on this value, glycerol films having a thickness $<1.5 \mu\text{m}$ will result in thermal diffusion lengths that are greater than the sample thickness and therefore allow for heat generated in the photoresist layer (in phase with the excitation light) via optical absorption to interact with the gas interface. In such cases in which the glycerol film is both optically and thermally thin, the observed photoacoustic spectra will exhibit absorption features characteristic of glycerol and photoresist. This effect can be seen in Figure 6 for the photoacoustic spectra collected for glycerol film thicknesses of 0.5 μm and 1.0 μm . Glycerol films having a thickness $>1.5 \mu\text{m}$ will result in thermal diffusion lengths that are less than the sample thickness and therefore allow for only heat generated in the glycerol film via optical absorption to interact with the gas interface. In such cases in which the glycerol film is both optically and thermally thick, the collected photoacoustic spectra will exhibit absorption features characteristic of glycerol only. This effect can be seen in Figure 6 for the photoacoustic spectra collected for a 2.5 μm glycerol film.

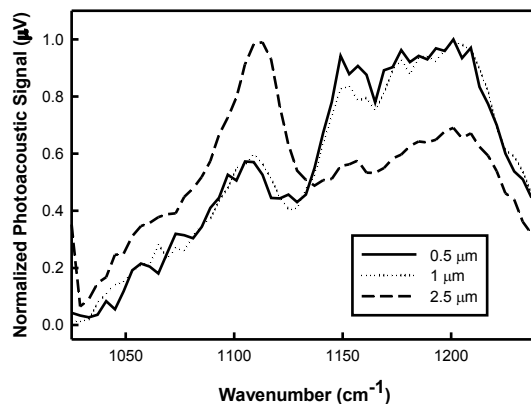


Figure 6. Laser photoacoustic spectral absorption features for varying thicknesses of glycerol films on a photoresist-coated silicon substrate collected at 12.5 kHz.

As the glycerol film thickness was increased, the magnitude of the absorption feature at $\sim 1100 \text{ cm}^{-1}$ (associated with the glycerol molecules) also increased. The opposite observation can be made for the broad absorption feature centered at $\sim 1175 \text{ cm}^{-1}$ (associated with the photoresist molecules). For thinner glycerol films, the magnitude and appearance of this broad feature were significant; however, as the glycerol film thickness increased, the magnitude of this absorption feature decreased. These results were due to the film thickness approaching the maximum diffusion length at 12.5 kHz.

A more comprehensive set of pulse repetition rates and precisely controlled sample thicknesses may result in improved analyte spectral differentiation. Nonetheless, the results for glycerol demonstrate the ability of this photoacoustic platform to accurately discriminate between species deposited on a surface.

5. CONCLUSION

We have successfully demonstrated a QCL-based PAS platform for the detection of condensed phase materials. Our results illustrate that this method can be used to collect quality infrared spectra of energetic analytes of interest, including urea and TNT, and for depth profiling analyses to distinguish among glycerol films deposited on photoresist-coated silicon wafers based on their laser photoacoustic spectra. The availability of continuously tunable QCLs having a broad wavelength and pulse or modulation frequency tuning range makes this an attractive approach for a variety of military and homeland defense applications.

ACKNOWLEDGEMENTS

The authors thank William Benard of the U.S. Army Research Laboratory for preparing the photoresist-coated silicon wafers and Bill Potter of the U.S. Army Research Laboratory for assistance with photoacoustic cell fabrication.

REFERENCES

- [1] J. S. Accetta and J. S. Baumgart, "Infrared reflectance spectroscopy and thermographic investigations of the Shroud of Turin," *Appl. Opt.* 19, 12, 1921 (1980).
- [2] P. J. Larkin, [IR and Raman Spectroscopy: Principles and Spectral Interpretation] Elsevier, Waltham, MA (2011).
- [3] S. E. Bialkowski, [Photothermal Spectroscopy Methods for Chemical Analysis] John Wiley & Sons, New York (1996).
- [4] A. K. Chaudhary, G. C. Bhar, and S. Das, "Low-limit photo-acoustic detection of solid RDX and TNT explosives with carbon dioxide laser," *J. Appl. Spectrosc.* 73, 1, 123 (2006).
- [5] A. Petzold and R. Niessner, "Photoacoustic soot sensor for in-situ black carbon monitoring," *Appl. Phys. B-Lasers Opt.* 63, 2, 191 (1996).
- [6] C. W. Van Neste, M. E. Morales-Rodriguez, L. R. Senesac, S. M. Mahajan, and T. Thundat, "Quartz crystal tuning fork photoacoustic point sensing," *Sens. Actuator B-Chem.* 150, 1, 402 (2010).
- [7] Q. Wen and K. H. Michaelian, "Mid-infrared photoacoustic spectroscopy of solids using an external-cavity quantum-cascade laser," *Opt. Lett.* 33, 16, 1875 (2008).
- [8] J. E. De Albuquerque, D. T. Balogh, and R. M. Faria, "Quantitative depth profile study of polyaniline films by photothermal spectroscopies," *Appl. Phys. A-Mater. Sci. Process.* 86, 3, 395 (2007).
- [9] K. Uchiyama, K. Yoshida, X. Z. Wu, and T. Hobo, "Open-ended photoacoustic cells: Application to two-layer samples using pulse laser-induced photoacoustics," *Anal. Chem.* 70, 3, 651 (1998).
- [10] M. H. Xu and L. H. V. Wang, "Photoacoustic imaging in biomedicine," *Rev. Sci. Instrum.* 77, 4, 041101 (2006).
- [11] F. G. C. Bijnen, J. Reuss, and F. J. M. Harren, "Geometrical optimization of a longitudinal resonant photoacoustic cell for sensitive and fast trace gas detection," *Rev. Sci. Instrum.* 67, 8, 2914 (1996).
- [12] F. J. M. Harren, F. G. C. Bijnen, J. Reuss, L. Voesenek, and C. Blom, "Sensitive intracavity photoacoustic measurements with a CO₂ wave-guide laser," *Appl. Phys. B-Photophys. and Laser Chem.* 50, 2, 137 (1990).
- [13] E. Holthoff, J. Bender, P. Pellegrino, and A. Fisher, "Quantum cascade laser-based photoacoustic spectroscopy for trace vapor detection and molecular discrimination," *Sensors* 10, 1986 (2010).
- [14] E. L. Holthoff, D. A. Heaps, and P. M. Pellegrino, "Development of a MEMS-scale photoacoustic chemical sensor using a quantum cascade laser," *IEEE Sens. J.* 10, 3, 572 (2010).
- [15] L. B. Kreuzer, "Laser optoacoustic spectroscopy - new technique of gas-analysis," *Anal. Chem.* 46, 2, A237 (1974).
- [16] A. Miklos and P. Hess, "Modulated and pulsed photoacoustics in trace gas analysis," *Anal. Chem.* 72, 30A (2000).
- [17] M. Nagele and M. W. Sigrist, "Mobile laser spectrometer with novel resonant multipass photoacoustic cell for trace-gas sensing," *Appl. Phys. B* 70, 895 (2001).
- [18] P. M. Pellegrino and R. G. Polcawich, "Advancement of a MEMS photoacoustic chemical sensor," *Proc. SPIE - Int. Soc. Opt. Eng.* 5085, 52 (2003).
- [19] C. W. Van Neste, L. R. Senesac, and T. Thundat, "Standoff photoacoustic spectroscopy," *Appl. Phys. Lett.* 92, 234102 (2008).
- [20] C. W. Van Neste, L. R. Senesac, and T. Thundat, "Standoff spectroscopy of surface adsorbed chemicals," *Anal. Chem.* 81, 1952 (2009).
- [21] L. B. Kreuzer, "Ultralow gas concentration infrared absorption spectroscopy," *J. Appl. Phys.* 42, 7, 2934 (1971).
- [22] L. B. Kreuzer, "The physics of signal generation and detection", in *Optoacoustic Spectroscopy and Detection*, Y.-H. Pao, Ed. (Academic Press, New York, 1977).
- [23] L. B. Kreuzer, N. D. Kenyon, and C. K. N. Patel, "Air-pollution - sensitive detection of 10 pollutant gases by carbon-monoxide and carbon-dioxide lasers," *Science* 177, 4046, 347 (1972).
- [24] A. Rosencwaig and A. Gersho, "Theory of photoacoustic effect with solids," *J. Appl. Phys.* 47, 1, 64 (1976).
- [25] A. C. Tam, "Photoacoustics: Spectroscopy and other applications", in *Ultrasensitive Laser Spectroscopy*, D. S. Klinger, Ed. (Academic Press, New York, 1983).
- [26] C. F. Dewey, Jr., "Design of optoacoustic system", in *Optoacoustic Spectroscopy and Detection*, Y.-H. Pao, Ed. (Academic Press, New York, 1977).
- [27] A. Miklos, P. Hess, and Z. Bozoki, "Application of acoustic resonators in photoacoustic trace gas analysis and metrology," *Rev. Sci. Instrum.* 72, 4, 1937 (2001).

- [28] J. Clarkson, W. E. Smith, D. N. Batchelder, D. A. Smith, and A. M. Coats, "A theoretical study of the structure and vibrations of 2,4,6-trinitrotoluene," *J. Mol. Struct.* 648, 203 (2003).
- [29] "NIST Standard Reference Database 69: NIST Chemistry Webbook, Urea". <http://webbook.nist.gov>.
- [30] J. A. Balderas-Lopez, A. Mandelis, and J. A. Garcia, "Measurements of the thermal diffusivity of liquids with a thermal-wave resonator cavity," *Anal. Sci.* 17, s519 (2001).

DEFENSE TECH INFO CTR
ATTN DTIC OCA (PDF)
8725 JOHN J KINGMAN RD STE 0944
FT BELVOIR VA 22060-6218

US ARMY RSRCH LAB
ATTN IMAL HRA MAIL & RECORDS MGMT
ATTN RDRL CIO LL TECHL LIB
ATTN RDRL CIO LT TECHL PUB
ATTN RDRL SEE E M FARRELL (3 COPIES)
ADELPHI MD 20783-1197